DOI: 10.19884/j.1672-5220.202509002

MOF-Supported Diimine-Ni Catalyzed Highly Active Propylene Dimerization

SONG Lulu, CHEN Long, SUN Junfen, LI Mingyuan*, WANG Le*, CAI Zhengguo*
State Key Laboratory of Advanced Fiber Materials, College of Materials Science and Engineering, Donghua University, Shanghai 201620, China

Abstract: A heterogeneous diimine-Ni catalyst (diimine-Ni@PCN-701) is synthesized through sequential ligand insertion into PCN-700, a robust Zr-based metal-organic framework (MOF), followed by chelation of Ni centers. This site-specific assembly affords a robust active center for propylene dimerization with superior activity, which arises from the electron-withdrawing effect of $Zr_6O_4(OH)_4$ clusters on the Ni active sites. Propylene is selectively converted into a series of dimers with 4-methyl-2-pentene (4M2P) as the main product, which may be due to the MOF structure promoting this reaction through both electronic effects and steric hindrance. This work highlights a general strategy for developing heterogeneous olefin oligomerization catalysts with high activity and shape selectivity through the precise construction of active sites.

Keywords: heterogeneous catalyst; metal-organic framework (MOF); diimine-Ni complex; propylene dimerization
CLC number: O632.12 **Document code**: A
Article ID: 1672-5220(2026)02-0043-08

Open Science Identity (OSID)

0 Introduction

Propylene is widely used as a monomer for producing polypropylene and ethylene-propylene rubbers[1]. With the rapid expansion of domestic propylene production in recent years, the synthesis of higher-value chemical propylene oligomers by using transition-metal catalysts has become an increasingly attractive yet challenging direction[2-6]. Among these processes, propylene dimerization produces a mixture of C6 olefin isomers, which serve as a critical building block for the industrial production of polymers and other chemicals[7-9].

Transition-metal catalysts offer unique opportunities as stereoselective olefin oligomerization catalysts, owing to their tunable ligand design[7, 10]. Among them, diimine-Ni catalysts have been demonstrated to efficiently promote olefin oligomerization, where the flexible structural tunability of diimine ligands further provides precisely adjustable coordination environments and high catalytic activity[11-12]. In contrast to homogeneous catalysts, heterogeneous catalysts offer longer lifetimes and easier product separation[13]. However, precise molecular-level control of active sites within solid supports still remains a major challenge[14]. Metal-organic frameworks (MOFs), with their well-defined coordination environments and tunable porosity, have emerged as promising platforms for heterogeneous catalysis[15-17].

Ni complexes immobilized on MOFs are especially appealing for propylene dimerization. However, most reported systems exhibit lower activity than their corresponding homogeneous counterparts in olefin dimerization[18-19], primarily due to limited control of the active-site environment and insufficient product regulation. Overcoming these challenges requires strategies that enable the precise construction of catalytic centers while simultaneously steering product selectivity. Mlinar et al.[20] prepared two Ni-based MOFs, Ni_2(dobdc) (dobdc^{4-} = 2,5-dioxido-1, 4-benzenedicarboxylate) and Ni_2(dobpdc) (dobpdc^{4-} = 4,4′-dioxido-[1,1′-biphenyl]-3,3′-dicarboxylate), with different pore sizes for propylene dimerization. The MOF structures impose distinct spatial and electronic environments on Ni^{2+} active sites, leading to different catalytic behaviors. The activity of these MOFs in catalyzing the gas-phase oligomerization of propylene is comparable to that of Ni^{2+}-exchanged aluminosilicates (Ni-Na-X[21] and Ni-Na-MCM-41[22]), with turnover frequency (TOF) values in a range of 10^2 to 10^3 h^{-1}.

Here, we report a heterogeneous diimine-Ni catalyst (denoted as diimine-Ni@PCN-701) synthesized via sequential ligand insertion into PCN-700 followed by Ni chelation[23-24]. This method allows the precise positioning of diimine-Ni sites within the MOF, while harnessing both the electron-withdrawing effect of Zr-based clusters[25-26] and the steric confinement[27-28]

Received date: 2025-09-04
Foundation items: National Natural Science Foundation of China (Nos. 22071023 and 22101056); Program of Shanghai Academic and Technology Research Leader, China (No. 22XD1400100); Fundamental Research Funds for the Central Universities, China (Nos. 2232020A-05 and 2232024D-04)
* Correspondence should be addressed to CAI Zhengguo, email: caizg@dhu.edu.cn; WANG Le, email: le.wang@dhu.edu.cn; LI Mingyuan, email: mingyuanli@dhu.edu.cn
Citation: SONG L L, CHEN L, SUN J F, et al. MOF-supported diimine-Ni catalyzed highly active propylene dimerization[J]. *Journal of Donghua University (English Edition)*, 2026, 43(2): 43-50.

provided by the MOF pores. As a result, the catalyst exhibits significantly enhanced activity compared with its molecular analogue and selectively produces 4-methyl-2-pentene (4M2P) as the major product, accounting for 57.6% of the total product, and exhibiting a TOF of 21 700 h^{-1}. This work establishes a general strategy for designing heterogeneous olefin dimerization catalysts with superior performance through the precise construction of active sites.

1 Materials and Methods

1.1 Materials

All solvents were distilled after being dried by sodium or purified by a solvent purification system (PS-MD-5, Innovative Technology, USA). Research-grade propylene was purified by a dehydration column of ZHD-20 and a deoxidation column of ZHD-20A. Dichloroethyl aluminum ($EtAlCl_2$) was purchased from Shanghai Energy Chemical Co., Ltd., China. Other commercially available reagents were purchased from Bide Pharmatech Ltd., China and used without further purification. Their purity and structural integrity were confirmed.

1.2 Synthesis of 2,2′-dimethyl-[1,1′-biphenyl]-4,4′-dicarboxylic acid (H_2Me_2-BPDC)

The ligand for PCN-700, H_2Me_2-BPDC, was synthesized following the procedure in Ref. [29] with slight modifications (Fig. 1). Methyl 4-iodo-3-methylbenzoate (5.00 mmol), bis(pinacolato)diboron (5.50 mmol), $Pd(dppf)Cl_2$ (dppf = 1,1′-bis(diphenylphosphino) ferrocene (0.15 mmol), and potassium acetate (CH_3COOK, 15.00 mmol) were added to a two-necked flask containing 30 mL *N*,*N*-dimethylformamide (DMF). The system was degassed by three freeze-pump-thaw cycles. The mixture was then heated at 80 ℃ in an oil bath and stirred for 12 h. After cooling, methyl 4-iodo-3-methylbenzoate (7.50 mmol), $Pd(dppf)Cl_2$ (0.15 mmol), sodium carbonate (Na_2CO_3, 25.00 mmol), and deionized water (12.5 g) were added to the reaction mixture. The system was again degassed and backfilled with nitrogen. The reaction was maintained at 80 ℃ for an additional 12 h. Upon completion, the mixture was extracted with diethyl ether, and the crude product was purified by flash column chromatography to afford dimethyl 2,2′-dimethylbiphenyl-4,4′-dicarboxylic acid dimethyl ester as a white solid.

The obtained white solid was subjected to hydrolysis under reflux in a 250 mL round-bottom flask containing 80 mL sodium hydroxide (NaOH, 2 mol/L) solution and 72 mL tetrahydrofuran (THF) for 12 h. The reaction mixture was acidified to pH = 2 with concentrated hydrochloric acid (HCl (aq)), extracted with THF, and concentrated under reduced pressure to afford H_2Me_2-BPDC.

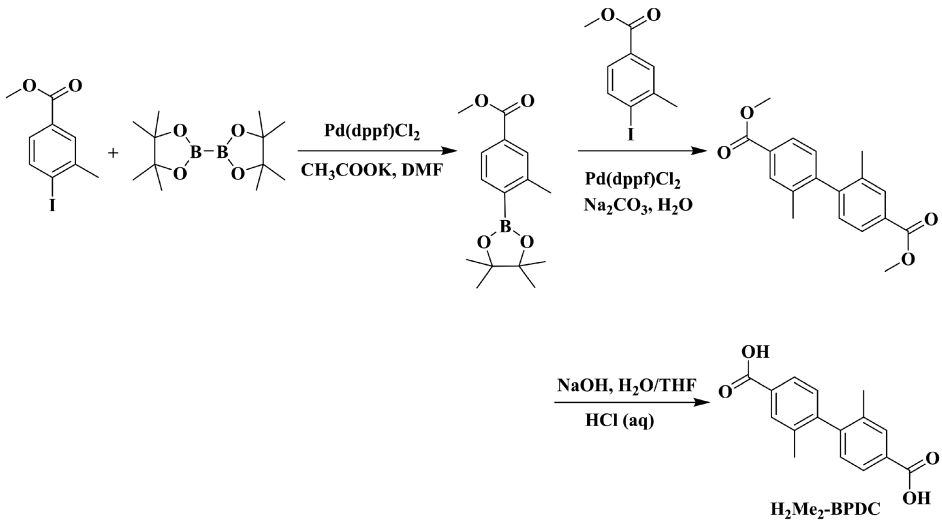

Fig. 1 Synthesis of H_2Me_2-BPDC

1.3 Synthesis of diimine-Ni@PCN-701

The synthesis of PCN-700 was improved based on the previous synthesis method in Ref. [23]. Zirconium tetrachloride ($ZrCl_4$, 200 mg) and H_2Me_2-BPDC (100 mg) were dissolved in 30 mL DMF under ultrasonication. Followed by the addition of trifluoroacetic acid (TFA, 71 μL), 2 mL aliquots were dispensed into 4 mL heat-resistant vials. The sealed vials were heated at 120 ℃ for 72 h. While still hot, the mother liquor was decanted, and the solids were washed with fresh DMF. The resulting product was further washed with acetonitrile (MeCN) and acetone under the same procedure, affording PCN-700 crystals. Terephthalic acid (TA) and a diimine linker were sequentially introduced into defect sites of different lengths in PCN-700, followed by chelation of Ni onto the diimine ligand to yield diimine-Ni @ PCN-701 (Fig. 2). The incorporation of TA stabilized the 12-connected pore structure, and the resulting pore volume was well aligned with the selective propylene dimerization confined within the designed framework.

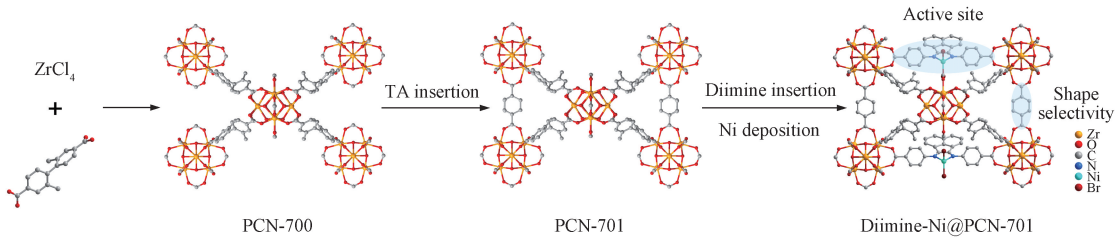

Fig. 2 Synthesis of diimine-Ni@PCN-701

1.4 General procedure for propylene dimerization

The dimerization reaction of propylene was carried out in a stainless steel high-pressure reactor. Before the dimerization reaction, the reactor was evacuated at 120 ℃ for 30 min, followed by repeated evacuation and nitrogen flushing. A certain amount of toluene, a specified number of equivalents of $EtAlCl_2$, and 1 μmol diimine-Ni@PCN-701 were added into the reactor under a nitrogen atmosphere. The total volume of the reaction system was 30 mL. At this point, stirring was initiated, and the catalytic system was activated for 10 min. Subsequently, high-purity propylene was introduced into the reactor to the desired reaction pressure (gauge pressure, corresponding to the propylene partial pressure) by using a precision pressure control system and was continuously supplied to maintain the pressure P throughout the dimerization reaction. After reaction for 10 min, the propylene valve was closed, and the reactor was cooled in liquid nitrogen. When the temperature of the reaction system dropped to −20 ℃, any residual propylene was slowly vented until the atmospheric pressure was achieved. The reactor was opened, and the reaction mixture was collected. To this mixture, 100 μL cooled cyclopentene as an internal standard was added. After thorough mixing, the solution was analyzed by gas chromatography-mass spectrometry (GC-MS). The product peaks of GC-MS were assigned according to the commercially available C6 isomer standard substances.

A SH-Alumina BOND/Na_2SO_4 capillary column (Shimadzu, Japan) (0.53 mm × 50 m, 10 μm film thickness) was used. The injection port was maintained at 200 ℃, with N_2 as the carrier gas at a flow rate of 10 mL/min. The column temperature was held at 30 ℃ for 3 min, then ramped to 180 ℃ at 10 ℃/min and held for 28 min. The injection volume was 1 μL with a split ratio of 10∶1.

1.5 Characterization

The morphologies of PCN-700 and diimine-Ni@PCN-701 were observed through an ultra-depth-of-field microscope (DVM6, Leica, Germany). Powder X-ray diffraction (PXRD) patterns of PCN-700 were tested by using an X-ray diffractometer (D8 ADVANCE, Bruker, Germany). X-ray photoelectron spectroscopy (XPS) data of diimine-Ni@PCN-701 were obtained by using a spectrometer (Escalab 250Xi, Thermo Scientific, USA) with an excitation source of Al-Ka radiation. The distribution of elements in diimine-Ni@PCN-701 was determined by using a scanning electron microscope and an energy dispersive spectroscope (GeminiSEM 560, ZEISS, Germany) operated at an accelerating voltage of 10 kV. The mass fractions of Zr and Ni in diimine-Ni@PCN-701 were determined by inductivity-coupled plasma optical emission spectroscopy (ICP-OES) using a spectrometer (Teledyne Leeman Prodigy Plus, Teledyne Leeman Labs, USA), with a wavelength range of 165–800 nm and a resolution of no more than 0.005 nm.

2 Results and Discussion

2.1 Characterization of PCN-700

PXRD confirms that the crystal structure of PCN-700 remains intact after sequential ligand and metal modifications (Fig. 3(a)). Ligand insertion induces an elongation of the framework along the crystallographic axis, leading to a slight shift of the diffraction peak near 7°, while the overall crystallinity is preserved. Compared with PCN-700, the overall crystallinity of diimine-Ni@PCN-701 is preserved. The oxidation state of Ni is verified by XPS. In the Ni 2p spectrum (Fig. 3(b)), the binding energies of Ni $2p_{3/2}$ and Ni $2p_{1/2}$ orbitals appear at 856.7 and 874.5 eV, respectively, accompanied by two pronounced satellite (sat.) peaks, indicating that Ni is anchored in the MOF in the form of positive divalent. The fine structure of diimine-Ni@PCN-701 has been analyzed in detail in previous studies[30].

The crystal morphologies of PCN-700 and diimine-Ni@PCN-701 were characterized by using an ultra-depth-of-field microscope. As shown in Fig. 3(c), PCN-700 appears as colorless and transparent crystals with a typical orthorhombic morphology, smooth surface, and uniform size. Following sequential ligand and metal incorporation, the crystals turn yellow while largely retaining their morphology and structure, although multiple modification steps partially disrupted the regular crystal form. Scanning electron microscopy and energy dispersive spectroscopy (SEM-EDS) mapping of diimine-Ni@PCN-701 (Fig. 3(d)) confirms that N and Ni from the diimine-Ni complex are homogeneously distributed throughout the MOF, demonstrating uniform active-site dispersion and a precisely controlled chemical environment. The mass fraction of Ni loading in the heterogeneous catalyst is determined by ICP-OES to be 2.76%.

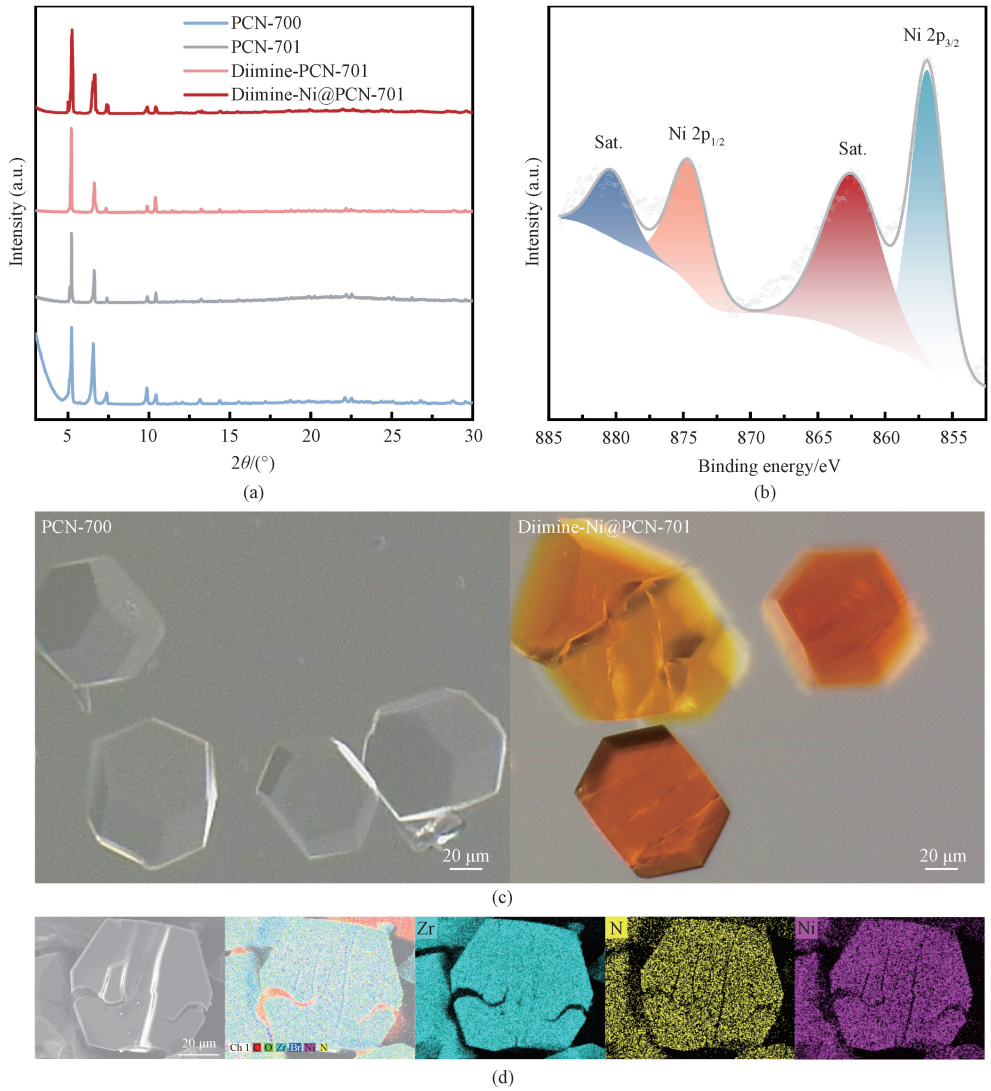

Fig. 3 Characterization of PCN-700 and diimine-Ni@PCN-701: (a) PXRD patterns of PCN-700, PCN-701, diimine-PCN-701 and diimine-Ni@PCN-701; (b) XPS spectrum of diimine-Ni@PCN-701; (c) ultra-depth-of-field microscopy images of PCN-700 and diimine-Ni@PCN-701; (d) SEM-EDS mapping of diimine-Ni@PCN-701

2.2 Catalytic property of diimine-Ni@PCN-701 for propylene dimerization

Propylene dimerization was catalyzed by using diimine-Ni @ PCN-701 with alkylaluminum as a cocatalyst, and the catalytic property was systematically evaluated under various reaction conditions. The corresponding dimerization results are summarized in Table 1.

Under the reaction conditions summarized in Table 1, diimine-Ni@PCN-701 exhibits 100% selectivity for propylene dimerization, with no detectable trimers or higher oligomers. Product yields are determined by gas chromatography using the internal standard method, based on the ratio of the integrated peak areas of the products to that of the standard. Catalytic activity is expressed as the TOF, defined as the moles of propylene converted per mole of Ni site per hour. It is confirmed that all Ni sites in the system areaccessible to the reactants.

Table 1 Propylene dimerization catalyzed by diimine-Ni@PCN-701

Entry	P/kPa	Al/Ni molar ratio	TOF/(h^{-1})	Molar ratio of each dimer in total amount of product/%								
				Path 1	Path 2			Path 3	Path 4			Isomerization
				2M1P	1H	*E*-2H	*Z*-2H	DM1B	4M1P	*E*-4M2P	*Z*-4M2P	2M2P
1[a]	100	100	5 700	1.7	3.5	16.3	5.0	0.8	15.4	50.9	6.0	0.4
2[a]	400	100	21 700	0.7	3.1	15.4	5.8	1.0	15.7	52.0	5.6	0.7
3[a]	700	100	36 500	2.1	3.0	16.7	5.5	1.2	17.2	46.6	5.8	1.9
4[a]	1 000	100	35 900	1.6	2.8	17.3	6.6	0.5	17.6	47.1	4.7	1.8
5[a]	400	200	33 200	2.1	3.5	16.2	5.4	2.4	16.4	45.9	5.8	2.3
6[a]	400	400	56 900	1.1	3.6	18.6	5.5	0.7	15.8	45.9	6.8	2.0
7[a]	400	600	50 300	0.0	3.8	15.8	4.0	0.7	17.8	51.4	6.5	0.0
8[b]	400	400	18 600	5.9	4.1	15.1	6.7	3.4	18.5	37.7	6.6	2.0
9[c]	400	400	15 200	4.9	1.6	13.3	6.2	6.7	14.5	31.6	7.0	14.2
10[d]	400	400	19 900	7.2	8.6	19.3	9.2	6.1	15.5	25.2	4.0	4.9

Notes: 2-methyl-1-pentene (2M1P); 1-hexene (1H); (*E*)-2-hexene (*E*-2H); (*Z*)-2-hexene (*Z*-2H); 2,3-dimethyl-1-butene (DM1B); 4-methyl-1-pentene (4M1P); (*E*)-4-methyl-2-pentene (*E*-4M2P); (*Z*)-4-methyl-2-pentene (*Z*-4M2P); 2-methyl-2-pentene (2M2P); [a]cocatalyst is $EtAlCl_2$; [b]cocatalyst is Et_2AlCl; [c]cocatalyst is methylaluminoxane (MAO); [d]catalyst is diimine-Ni.

The propylene dimerization pathways are shown in Fig. 4. As illustrated in Fig. 4, propylene dimerization proceeds via two consecutive insertions at the Ni active center. The regioselectivity of each insertion step (1, 2-insertion or 2, 1-insertion) gives rise to four distinct reaction pathways (paths 1 – 4). The product distribution indicates that the dominant pathway involves two consecutive 2, 1-insertions (path 4), yielding a mixture of 4 M1P and 4 M2P. Under certain conditions, *E*-4M2P accounts for more than 50% of the total products. The only isomerization product observed is 2M2P, which is an isomer of the main dimerization products, consistent with the overall dimerization pathways.

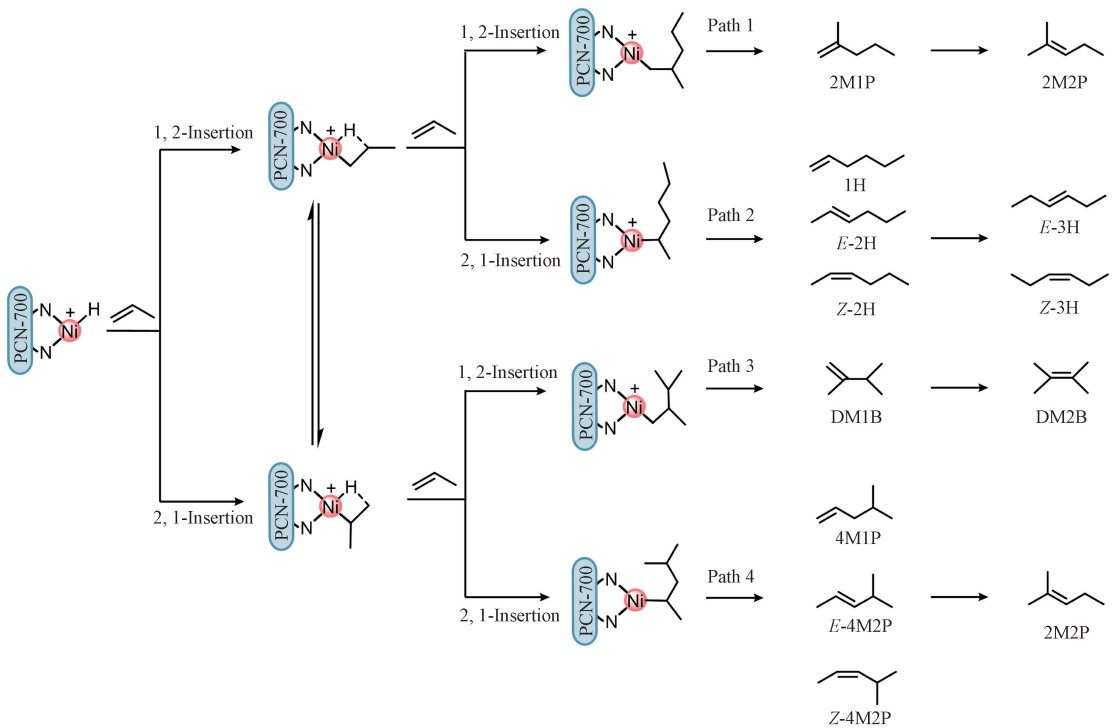

Fig. 4 Propylene dimerization pathways

At low propylene concentrations, the TOF increases linearly with the propylene pressure in a range of 100 – 700 kPa (entries 1 – 3 in Table 1). The activity plateaus beyond 700 kPa (entry 4 in Table 1), suggesting that the reaction is limited by monomer availability at low propylene concentrations, whereas at higher propylene concentrations, mass-transfer limitations dominate. Product distribution is only slightly affected, with a

minor increase in isomerization at higher propylene concentrations.

The Al/Ni molar ratio has a significant influence on the performance of propylene dimerization (entries 1 and 5–7 in Table 1). Figure 5 presents the gas chromatogram of the dimer products obtained under the reaction conditions corresponding to entry 5, with the isomer type corresponding to each chromatographic peak labeled in Fig. 5. The optimal Al/Ni molar ratio for propylene dimerization is 400, yielding the highest TOF of 56 900 h^{-1}. Increasing the Al/Ni molar ratio increases the proportion of products along path 3. The products along path 4 account for 75.7% of the total products when the Al/Ni molar ratio is 600, while isomerized products are nearly eliminated.

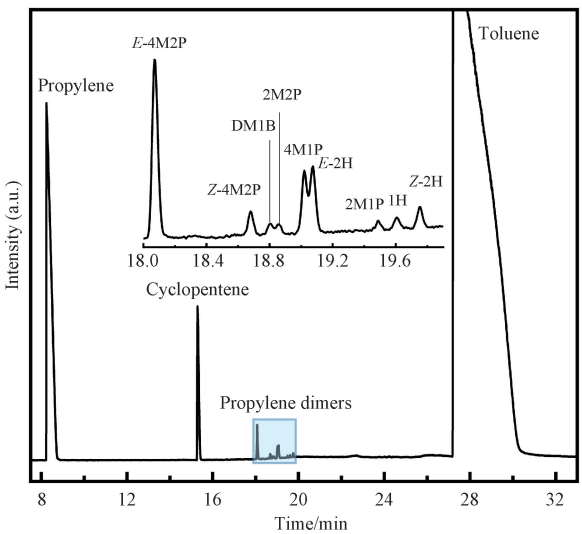

Fig. 5 Typical gas chromatogram of propylene dimerization catalyzed by diimine-Ni@PCN-701 (cocatalyst is $EtAlCl_2$, Al/Ni molar ratio is 200, T=0 ℃, and P=400 kPa)

The properties of the cocatalyst also play a crucial role. Using Et_2AlCl_2 instead of $EtAlCl_2$ results in significantly lower activity (entries 6 and 8 in Table 1), reflecting its weaker Lewis acidity, which necessitates a longer induction period for activation of the Ni center by the cocatalyst. However, despite its stronger Lewis acidity, MAO exhibits lower activity under the same conditions (entry 9 in Table 1), likely due to diffusion limitations of the bulk polymer within the MOF pores. However, the proportion of the isomerized product (2M2P) increases significantly when MAO is used as a cocatalyst, which still primarily originates from path 4.

After the dimerization reaction, the supernatant was filtered and collected, and the concentrations of Zr and Ni in the concentrated supernatant were measured by ICP-OES. The results show that no Zr or Ni is detected, indicating that no metal leaching occurred during the entire reaction process and that propylene dimerization proceeded under heterogeneous conditions.

As expected, diimine-Ni@PCN-701 exhibits higher dimerization activity than the corresponding molecule diimine-Ni catalyst (56 900 h^{-1} vs. 19 900 h^{-1}). This result stems from the strong electron-withdrawing ability of the $Zr_6O_4(OH)_4$ clusters, which reduces the electron density at the Ni center and accelerates the rate of propylene coordination insertion. Meanwhile, the dimerization products of the homogeneous system contain a higher proportion of linear dimer products (path 2), demonstrating the significant influence of the support on catalytic performance.

3 Conclusions

A heterogeneous Ni catalyst was synthesized by immobilizing molecular diimine-Ni into PCN-700 and effectively promoted propylene dimerization under mild conditions. Compared to its homogeneous diimine-Ni counterpart, this heterogeneous catalyst exhibited markedly enhanced activity with 4M2P selectivity of 57.6% among the oligomer products. The improved catalytic performance can be attributed to electronic modulation imposed by the distal zirconium clusters of the MOF, which alter the electronic environment of the diimine ligand to facilitate more efficient catalysis.

References

[1] PHUNG T K, LE MINH PHAM T, VU K B, et al. (Bio) propylene production processes: a critical review [J]. *Journal of Environmental Chemical Engineering*, 2021, 9(4): 105673.

[2] MAGAZOVA G, CHO Y, MUHLENKAMP J A, et al. Single-site, Ni-modified Wells-Dawson-type polyoxometalate for propylene dimerization [J]. *Catalysis Science & Technology*, 2022, 12(19): 5970-5981.

[3] LING Y, CHEN X, TONG H K, et al. Modulating the interaction of $NiSO_4$ and Nb_2O_5 boosts the dimerization of propylene [J]. *Industrial & Engineering Chemistry Research*, 2021, 60(19): 6959-6970.

[4] LIU L, LIU Z, CHENG R H, et al. Ligand-induced product switching between 4-methyl-1-pentene and 2-methyl-1-pentene in bis(imino) pyridine/V(III)-catalyzed propylene dimerization: cossee-arlman versus metallacycle mechanism [J]. *Organometallics*, 2021, 40(11): 1682-1691.

[5] WU S Z, LU S W. Propylene dimerization by $(\eta^5\text{-}C_9H_7)_2$ nickel (II) catalytic system [J]. *Chinese Journal of Chemistry*, 2003, 21(4): 372-376.

[6] YEH B, CHHEDA S, PRINSLOW S D, et al. Structure and site evolution of framework Ni species in MIL-127 MOFs for propylene oligomerization catalysis [J]. *Journal of the American Chemical Society*, 2023, 145(6):

3408-3418.
[7] OLIVIER-BOURBIGOU H, BREUIL P R, MAGNA L, et al. Nickel catalyzed olefin oligomerization and dimerization[J]. *Chemical Reviews*, 2020, 120(15): 7919-7983.
[8] CHEN P, LING Y, TONG H K, et al. From propylene to 4-methyl-1-pentene over K-Cu supported catalytically active liquid metal solutions[J]. *ChemistrySelect*, 2023, 8(45): e202303724.
[9] DEIMUND M A, LABINGER J, DAVIS M E. Nickel-exchanged zincosilicate catalysts for the oligomerization of propylene[J]. *ACS Catalysis*, 2014, 4(11): 4189-4195.
[10] PENG A F, HUANG Z, LI G. Ethylene oligomerization catalyzed by different homogeneous or heterogeneous catalysts [J]. *Catalysts*, 2024, 14(4): 268.
[11] KILLIAN C M, JOHNSON L K, BROOKHART M. Preparation of linear α-olefins using cationic nickel (II) α-diimine catalysts [J]. *Organometallics*, 1997, 16(10): 2005-2007.
[12] SVEJDA S A, BROOKHART M. Ethylene oligomerization and propylene dimerization using cationic (α-diimine) nickel (II) catalysts [J]. *Organometallics*, 1999, 18(1): 65-74.
[13] SEUFITELLI G V S, RESENDE F L P. Study of the catalytic reactions of ethylene oligomerization in subcritical and supercritical media over a NiBEA catalyst [J]. *Applied Catalysis A: General*, 2019, 576: 96-107.
[14] OLIVIER-BOURBIGOU H, FORESTIÈRE A, SAUSSINE L, et al. Olefin oligomerization for the production of fuels and petrochemicals[J]. *Oil Gas European Journal*, 2010, 36(2), 97-102.
[15] COHEN S M. Postsynthetic methods for the functionalization of metal-organic frameworks [J]. *Chemical Reviews*, 2012, 112(2): 970-1000.
[16] WEI Y S, ZHANG M, ZOU R Q, et al. Metal-organic framework-based catalysts with single metal sites[J]. *Chemical Reviews*, 2020, 120(21): 12089-12174.
[17] JIAO L, WANG Y, JIANG H L, et al. Metal-organic frameworks as platforms for catalytic applications[J]. *Advanced Materials*, 2018, 30(37): 1703663.
[18] LIU L J, DAVID HARRIS T. Metal-organic frameworks as potential catalysts for industrial 1-butene production[J]. *ACS Central Science*, 2016, 2(3): 125-127.
[19] COMITO R J, METZGER E D, WU Z, et al. Selective dimerization of propylene with Ni-MFU-1[J]. *Organometallics*, 2017, 36(9), 1681-1683.
[20] MLINAR A N, KEITZ B K, GYGI D, et al. Selective propene oligomerization with nickel(II)-based metal-organic frameworks [J]. *ACS Catalysis*, 2014, 4(3): 717-721.
[21] MLINAR A N, BAUR G B, BONG G G, et al. Propene oligomerization over Ni-exchanged Na-X zeolites[J]. *Journal of Catalysis*, 2012, 296: 156-164.
[22] MLINAR A N, SHYLESH S, HO O C, et al. Propene oligomerization using alkali metal- and nickel-exchanged mesoporous aluminosilicate catalysts[J]. *ACS Catalysis*, 2014, 4(1): 337-343.
[23] YUAN S, LU W G, CHEN Y P, et al. Sequential linker installation: precise placement of functional groups in multivariate metal-organic frameworks [J]. *Journal of the American Chemical Society*, 2015, 137(9): 3177-3180.
[24] YUAN S, ZHANG P, ZHANG L L, et al. Exposed equatorial positions of metal centers via sequential ligand elimination and installation in MOFs[J]. *Journal of the American Chemical Society*, 2018, 140(34): 10814-10819.
[25] WISSER F M, BERRUYER P, CARDENAS L, et al. Hammett parameter in microporous solids as macroligands for heterogenized photocatalysts [J]. *ACS Catalysis*, 2018, 8(3): 1653-1661.
[26] KAJIWARA T, FUJII M, TSUJIMOTO M, et al. Photochemical reduction of low concentrations of CO_2 in a porous coordination polymer with a ruthenium(II)-CO complex[J]. *Angewandte Chemie (International Ed)*, 2016, 55(8): 2697-2700.
[27] METZGER E D, BROZEK C K, COMITO R J, et al. Selective dimerization of ethylene to 1-butene with a porous catalyst[J]. *ACS Central Science*, 2016, 2(3): 148-153.
[28] METZGER E D, COMITO R J, WU Z W, et al. Highly selective heterogeneous ethylene dimerization with a scalable and chemically robust MOF catalyst[J]. *ACS Sustainable Chemistry & Engineering*, 2019, 7(7): 6654-6661.
[29] CASTNER A T, JOHNSON B A, COHEN S M, et al. Mimicking the electron transport chain and active site of [FeFe] hydrogenases in one metal-organic framework: factors that influence charge transport[J]. *Journal of the American Chemical Society*, 2021, 143(21): 7991-7999.
[30] SONG L L, UNIVERSITY D, CHEN L, et al. MOF-supported diimine nickel catalyst for highly active and selective ethylene dimerization [J]. *ACS Catalysis*, 2025, 15(15): 12590-12597.

MOF 负载二亚胺镍催化高活性丙烯二聚反应

宋璐璐，陈　龙，孙俊芬，李明远*，王　乐*，蔡正国*
东华大学 先进纤维材料全国重点实验室，材料科学与工程学院，上海 201620

摘　要：通过在 Zr 基金属有机骨架（metal-organic framework，MOF）PCN-700 中进行顺序配体插入，螯合 Ni 活性中心的方法合成了一种非均相二亚胺镍催化剂（diimine-Ni@PCN-701）。得益于 $Zr_6O_4(OH)_4$ 簇对 Ni 活性位点的吸电子效应，该位点特异性组装体为丙烯二聚反应提供了稳定的活性中心，并具有优异的活性。丙烯选择性地转化为以 4-甲基-2-戊烯作为主要产物的一系列二聚体，这可能是由于 MOF 的结构在电子效应和空间位阻上共同促进了这一反应。本研究提出了一种通过精确构建活性位点来开发具有高活性和形状选择性的非均相烯烃齐聚催化剂的通用策略。

关键词：非均相催化剂；金属有机骨架（MOF）；二亚胺镍配合物；丙烯二聚